Towards Tandem Photovoltaic Devices Employing Nanoarray Graphene-based Sheets

—Supplementary Information

Yongfu Zhu, Ning Zhao, Jianshe Lian, Qing Jiang

Key Laboratory of Automobile Materials (Jilin University), Ministry of Education, and School of Materials Science and Engineering, Jilin University, Changchun, 130022, China

1. Way to explore E_c^M

Since the difference in E_c^M concerning with the interface geometrical structure is negligibly small,[1] the values of $E_{C=C}$ and $E_{C\text{-}M}$ for the calculation will be taken from the zigzag-structured interface here. With reference to Singh,[1] $E_{C\text{-}M}$ and $E_{C=C}$ with M = BN here will be calculated by the simulation method using ZZ-GNRs embedded in M with M = BN through $E_{C\text{-}M} = (E_{total} - E_{GNR} - E_M)/n_1$ and $E_{C=C} = (E_{total} - E_M - n_1E_C - n_1E_{C\text{-}M} - E_{C\text{-}part})/n_2$. In these expressions, E_{total} denotes the total energy of the whole system, E_{GNR} the energy of the GNR part, and E_M the energy of M part after removing the GNR part from the whole system, n_1 the number of broken bonds between the embedded GNR and M at the interface, E_C the energy of the edge C atom in the GNR part bonded to M at the interface, $E_{C\text{-}part}$ the energy of the left C part that double bonded to the edge C atoms of the embedded GNRs, and n_2 the number of the broken C=C bonds at the edges of GNRs. In view of it, the parameters of E_{total}, E_{GNR}, E_M, E_C and $E_{C\text{-}part}$ should be given. To have these parameters, the spin-polarized DFT calculations are performed using DMol^3 code.[2,3] The GGA with PBE is employed as the exchange correlation functional.[2] Double numeric plus polarization and all-electron core treatment are adopted for all calculations.

2. $E_g(D)$ as the function of the physiochemical amount α_{2D}^M

To reveal the essential reason for the distinction in the BOs regarding the edge geometrical structure and the host material, Figure S1 shows the $E_g(D)$ plot of GQDs/M at D = 1.6 nm as specified by the physiochemical amount α_{2D}^M along the x-axis. $E_g(D)$ decreases as α_{2D}^M shrinks for GQDs/M, where $E_g(D)$ of the AC structure is larger than that of the ZZ case. The reason for this is that the C atoms at the AC edge are less stable than those at the ZZ edge because of the homogeneous/inhomogeneous repulsion along the ZZ/AC edges, while α_{2D} can denote such a difference in the present investigation associated with the chemical bonding of edge-C atoms.[4,5] On the other hand, when M is transformed from BN to GA, $E_g(D)$ is ranged from 0.70 to 0.84 eV for the ZZ-structured interface and from

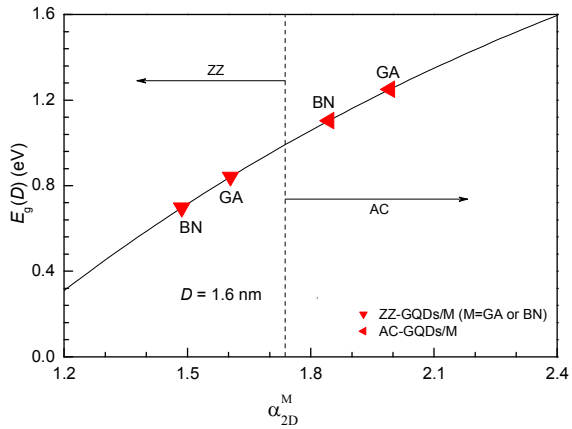

Figure S1 $E_g(D)$ of GQDs/M as the function of the physiochemical amount α_{2D}^{M} at D = 1.6 nm.

1.10 to 1.25 eV for the AC-structured case. This result suggests that the host material can also affect the BOs in GQDs/M, which should be essentially attributed to the different atomic cohesive energy of interface-C atoms concerning with the roles played by the host material.

3. Difference in $E_g(D)$ as the function of L assessed between the GGA-PBE method and the hybrid sX-LDA functional

3.1 $E_g(D)$ as the function of L simulated with the GGA-PBE method

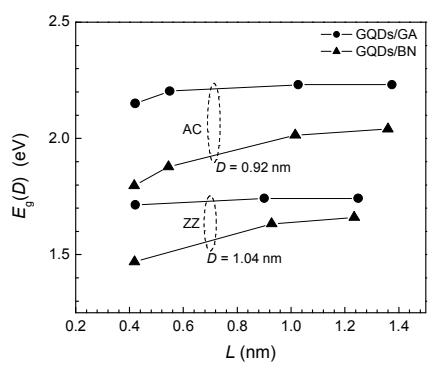

Figure S2 A simulation on $E_g(D)$ as the function of L with the GGA-PBE method for GQDs/GA and GQDs/BN at D = 0.92 nm for the AC-structured interface or D = 1.04 nm for the ZZ-structured interface.

Figure S2 shows $E_g(D)$ as the function of L obtained with the GGA-PBE simulation method. The $E_g(D)$ size depends largely on the host materials and the interface structure, decreasing in the order AC-GQDs/GA, AC-GQDs/BN, ZZ-GQDs/GA and ZZ-GQDs/BN. When M = GA, a slight decrease in $E_g(D)$ from 2.23 to 2.15 eV occurs for the AC-structured interface when L shrinks below 0.55 nm, while the change is hardly observed at larger L. $E_g(D)$ changes little in the range at 1.71 ~ 1.74 eV for the ZZ-structured interface. In the case with M = BN, in contrast, an obvious decrease in $E_g(D)$ can be observed from 2.04 to 1.80 eV for the AC-structured interface and from 1.66 to 1.47 eV for the ZZ-structured interface especially when L < 1.02 for the former and L < 0.93 nm for the latter.

3.2 Difference in $E_g(D)$ assessed between the GGA-PBE method and the hybrid sX-LDA functional

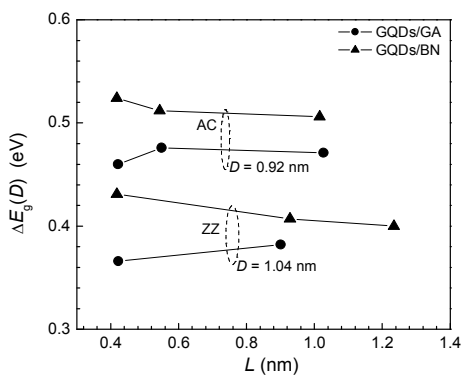

Figure S3 The difference in $E_g(D)$ assessed between the GGA-PBE method and the hybrid sX-LDA functional denoted with $\Delta E_g(D) = E_g(D)_{\text{sX-LDA}} - E_g(D)_{\text{GGA-PBE}}$.

It is generally known that the GGA-PBE method usually underestimates the band gap values.[6] In contrast, the values generated from the hybrid sX-LDA functional is more accurate comparable to those experiment results.[7,8] To evaluate the errors from the GGA-PBE method in this work, the difference in $E_g(D)$ between the GGA-PBE method and the hybrid sX-LDA functional were plotted as the function of L for AC(ZZ)-GQDs/M with $\Delta E_g(D) = E_g(D)_{\text{sX-LDA}} - E_g(D)_{\text{GGA-PBE}}$. Here, $E_g(D)_{\text{sX-LDA}}$ is taken from Figure 5 given in the paper, while $E_g(D)_{\text{GGA-PBE}}$ is from Figure S2. As shown in Figure S3, $\Delta E_g(D)$ varies in the range between 0.35 ~ 0.55 eV, while it

depends largely on the host materials and the interface geometrical structure, decreasing in the order of AC-GQDs/BN, AC-GQDs/GA, ZZ-GQDs/BN and ZZ-GQDs/GA. As each $\Delta E_g(D)$ curve is concerned, in addition, $\Delta E_g(D)$ increases slightly as L declines for AC-GQDs/BN and ZZ-GQDs/BN, although it decreases suddenly as L is decreased to 0.42 nm for AC-GQDs/GA and ZZ-GQDs/GA. However, the rangeability values of all $\Delta E_g(D)$ curves are limited only at 0.02~0.03 eV, suggesting that the influence of L on $\Delta E_g(D)$ is negligibly small.

In light of Figure S3, there exist obvious errors with the GGA-PBE method concerning with the host materials and the interface geometrical structure. This suggests that the hybrid sX-LDA functional should be adopted to check the influence from the crystalline field couple.

(1) Singh, A. K.; Penev, E. S.; Yakobson, B. I. Vacancy Clusters in Graphane as Quantum Dots. *ACS Nano* **2010,** *4*, 3510-3514.

(2) Delley, B. An All-Electron Numerical Method for Solving the Local Density Functional for Polyatomic Molecules. *J. Chem. Phys.* **1990,** *92*, 508-517.

(3) Delley, B. From Molecules to Solids with the Dmol[Sup 3] Approach. *J. Chem. Phys.* **2000,** *113*, 7756-7764.

(4) Sun, C. Q.; Fu, S. Y.; Nie, Y. G. Dominance of Broken Bonds and Unpaired Nonbonding Pi-Electrons in the Band Gap Expansion and Edge States Generation in Graphene Nanoribbons. *J. Phys. Chem. C* **2008,** *112*, 18927-18934.

(5) Silva, A. M.; Pires, M. S.; Freire, V. N.; Albuquerque, E. L.; Azevedo, D. L.; Caetano, E. W. S. Graphene Nanoflakes: Thermal Stability, Infrared Signatures, and Potential Applications in the Field of Spintronics and Optical Nanodevices. *J. Phys. Chem. C* **2010,** *114*, 17472-17485.

(6) Li, X.; Wu, X.; Zeng, X. C.; Yang, J. Band-Gap Engineering Via Tailored Line Defects in Boron-Nitride Nanoribbons, Sheets, and Nanotubes. *ACS Nano* **2012,** *6*, 4104-4112.

(7) Seidl, A.; Görling, A.; Vogl, P.; Majewski, J. A.; Levy, M. Generalized Kohn-Sham Schemes and the Band-Gap Problem. *Phys. Rev. B* **1996,** *53*, 3764-3774.

(8) Lee, B.; Wang, L.-W.; Spataru, C. D.; Louie, S. G. Nonlocal Exchange Correlation in Screened-Exchange Density Functional Methods. *Phys. Rev. B* **2007,** *76*, 245114.